Received: 8 July 2024 | Revised: 25 September 2024 | Accepted: 23 October 2024

DOI: 10.1111/aab.12962

Annals of Applied Biology
An international journal of the aab
WILEY

ORIGINAL ARTICLE

Identification and characterisation of *Zucchini yellow fleck virus* and a novel *Nepovirus* from next-generation sequencing of mixed virus infections in cucumbers (*Cucumis sativus*) from Crete

Anthony James[1] | Nikoleta Kryovrysanaki[1] | Christos Andronis[1] | Polyxeni G. Pappi[2] | Kriton Kalantidis[1,3] | Konstantina Katsarou[1,3]

[1]Institute of Molecular Biology and Biotechnology, Foundation for Research and Technology-Hellas, Heraklion, Greece

[2]Laboratory of Plant Virology, Department of Viticulture, Vegetable Crops, Floriculture and Plant Protection, Institute of Olive Tree, Subtropical Crops and Viticulture, Hellenic Agricultural Organization – "DIMITRA", Heraklion, Greece

[3]Department of Biology, University of Crete, Voutes University Campus, Heraklion, Greece

Correspondence
Konstantina Katsarou and Kriton Kalantidis, Institute of Molecular Biology and Biotechnology, Foundation for Research and Technology-Hellas, Heraklion, Crete, Greece.
Email: katsarou@imbb.forth.gr and kriton@imbb.forth.gr

Present address
Anthony James, Centre for Agriculture and the Bioeconomy, Queensland University of Technology, Brisbane, Australia.

Funding information
European Union- Next Generation EU, Greece 2.0 National Recovery and Resilience plan; General Secretariat of Research and Technology - Greece

Abstract

Cucumbers are susceptible to infections with many characterised virus species. In some cases, mixed virus infections occur and produce novel symptoms. In Greece, routine screening is carried out when virus infection is suspected, or novel symptoms are observed in the field. To identify the viruses associated with distinct symptoms observed in samples from commercial cucumber production areas on the island of Crete, Greece, we carried out high-throughput sequencing (HTS) from a pool of six samples. Following assembly and BLAST analysis, we identified at least seven viruses based on similarity to published sequences. Two of these sequences represented novel, near-complete genomes of a putative new nepovirus and of zucchini yellow fleck virus (ZYFV). To confirm the HTS results, the six samples were screened for all identified viruses, and their presence was confirmed through Sanger sequencing of PCR products. The full-length genomes of both the nepovirus and ZYFV were amplified by PCR and confirmed by Sanger sequencing. We have generated the complete genome of a novel nepovirus from cucumber as well as the first complete genome sequence of a cucumber-infecting ZYFV isolate from Crete. The nepovirus was mechanically transmissible to *Nicotiana benthamiana* and induced typical cytopathological modifications consistent with virus infection, as revealed by TEM studies. We propose to name this new virus Cucumber nepovirus A (CuNVA).

KEYWORDS
cucurbit, high-throughput sequencing, mixed infections, nepovirus, plant virus, potyvirus

1 | INTRODUCTION

Cucumber (*Cucumis sativus* L.) is a member of the *Cucurbitaceae* family, which includes several other important crop plants such as melon,

---

Anthony James and Nikoleta Kryovrysanaki these authors contributed equally to this work.

pumpkin and squash. Cucumbers are cultivated worldwide, mostly as seasonal vegetable crops, with 2.3 million hectares (ha) cultivated in 2022, producing approximately 91 million tons (https://www.fao.org/faostat/en/#data/QCL). China is the largest producer, followed by Turkey, Russia and Iran. Cucumber production in Greece is relatively small, with only 1980 ha cultivated, producing 159,000 tons in 2020, with the island of Crete being the leading production region.

Worldwide, viruses from several different families have been identified infecting cucumbers (Desbiez, 2020). The most well-known of these is Cucumber mosaic virus (CMV), with a very large host range including cultivated and wild cucurbits (Palukaitis et al., 1992). Other important cucurbit-infecting viruses include Artichoke yellow ringspot virus (AYRSV, genus *Nepovirus*), beet pseudo-yellows virus (BPYV, genus *Crinivirus*), cucurbit aphid-borne yellows virus (CABYV, genus *Polerovirus*), cucurbit chlorotic yellows virus (CCYV, genus *Crinivirus*), cucumber green mottle mosaic virus (CGMMV, genus *Tobamovirus*), cucurbit vein yellowing virus (CVYV, genus *Ipomovirus*), cucurbit yellow stunting disorder virus (CYSDV, genus *Crinivirus*), Moroccan watermelon mosaic virus (MWMV, genus *Potyvirus*), papaya ringspot virus (PRSV, genus *Potyvirus*), squash mosaic virus (SqMV, genus *Comovirus*), tomato leaf curl New Delhi virus (ToLCNDV, genus *Begomovirus*), watermelon mosaic virus (WMV, genus *Potyvirus*), zucchini yellow fleck virus (ZYFV, genus *Potyvirus*) and zucchini yellow mosaic virus (ZYMV, genus *Potyvirus*) (reviewed in Desbiez, 2020). Several viruses, including CGMMV, CCYV, AYRSV and WMV have previously been identified in Greece, including Crete (Avgelis, 1983; Avgelis & Vovlas, 1986; Avgelis & Vovlas, 1989; Orfanidou et al., 2014).

Various members of the family *Potyviridae* infect cucurbits in different parts of the world (Yang et al., 2021). ZYFV was first reported from zucchini in Italy (Vovlas et al., 1981), with flexuous particles of 700–800 nm observed in plants, together with inclusion bodies typical of potyviruses, observed in the cells of leaves from infected plants. ZYFV caused pinpoint yellow spot symptoms on the leaves of infected plants, which coalesced to form yellow flecks and blotches and later spread and became necrotic, and was transmitted by aphids as well as mechanically. ZYFV was subsequently reported from Greece, predominantly affecting the perennial weed squirting cucumber (*Ecballium elaterium* A. Rich.), but also in cucumber and melon crops (Avgelis, 1985). Symptoms of squirting cucumber included a mild mosaic, while in cucumbers distorted fruits were produced and yield/marketability was reduced. In contrast, melon cv. Galia showed severe symptoms including fruit deformation and plant death. ZYFV was later detected in Lebanon and Syria (Katul & Makkouk, 1987), France (Gilbert-Albertini & Lecoq, 1994), Israel (Antignus et al., 1995) and Iran (Bananej & Vahdat, 2008). Sequence analysis of the CP-coding region subsequently confirmed ZYFV as a distinct species within the PRSV-subgroup of the genus *Potyvirus* (Desbiez et al., 2007). At least eight distinct members are now associated with the PRSV subgroup in the genus *Potyvirus*, and full-length sequences have been characterised for most of these, including several complete genomes of ZYFV from Greece and Italy recently (Sareli et al., 2022).

A second important viral family with members infecting cucumbers and other cucurbits is the *Secoviridae*, with five distinct members of the genus *Nepovirus* identified in cucurbits to date. These include AYRSV (Avgelis & Vovlas, 1989), melon mild mottle virus (MMMoV) (Tomitaka et al., 2011), tobacco black ring virus (TBRV) (Gan et al., 2013), tobacco ringspot virus (TRSV) (Moore & McGuire, 1968) and tomato ringspot virus (ToRSV) (Chu et al., 1983). Nepoviruses (nematode-transmitted polyhedral viruses) were among the first 16 groups to be recognised by the International Committee on Taxonomy of Viruses (ICTV) in 1971 (Harrison et al., 1971). These viruses are usually transmitted by nematodes, although other possible vectors including insects, such as thrips, and mites have also been identified (Sanfaçon, 2008). Nepoviruses are small, non-enveloped, icosahedral viruses of ~30 nm diameter with a bipartite genome. Their genomic RNAs are covalently bound to a small protein called VPg (2–3 kDa) at the 5′ end and have a polyA tail at the 3′ end. Both RNAs encode for polyproteins, which are processed by a viral-encoded protease (3CL-PRO) at specific sites. RNA1 encodes an X1 protein of unknown function, an X2 protein possibly associated with replication, an NTP-binding protein (NTB), which constitutes the helicase of the virus, VPg, 3CL-PRO and the RNA-dependent RNA polymerase protein (POL) (Fuchs et al., 2017; Sanfaçon, 2022). The 5′ region of RNA2 encodes either one protein, named 2a, required for replication of RNA2, or two proteins named X3 and X4, of unknown function, followed by the movement protein (MP) and capsid protein (CP) (Fuchs et al., 2017; Sanfaçon, 2022). Nepoviruses are grouped into three subgroups (designated A, B and C), based on genome organisation and sequence identity (Sanfaçon, 2008; Sanfaçon, 2022). An interesting feature of nepovirus infections is the presence of satellite RNAs associated with several members of the genus, which hijack both the viral replication system as well as the capsid protein for movement (Sanfaçon, 2008).

Commercial cucumber production in Crete is hampered by several common virus diseases, for which routine diagnostic screening is undertaken. At times, symptomatic cucumber plants are observed in the field, however routine screening targets only a limited number of common viruses, including CMV, CCYV, CYSDV, BPYV and potyviruses. In 2019, six samples from plants showing severe yellowing, leaf size reduction, chlorotic patterns and spots, vein yellowing, and mosaic were collected and subjected to pooled high-throughput sequencing (HTS) to identify any viruses present. Based on the contigs present in the assembly of small reads at least seven distinct virus species were identified. One of these sequences had high similarity with the nepovirus artichoke Italian latent virus (AILV) but appeared to be a novel sequence, while a second sequence was a near complete genome of ZYFV, for which no complete genome was reported at the time of the study. Here we report the analysis of the HTS results including the characterisation of a novel nepovirus and the first complete genome sequence of a ZYFV isolate from cucumber.

2 | MATERIALS AND METHODS

2.1 | Next-generation sequencing and virus identification

RNA was extracted from leaf tissue using the Spectrum™ Plant Total RNA Kit (Sigma-Aldrich) and 350 ng of RNA from each sample was pooled. HTS was carried out at Macrogen Europe (Amsterdam, The Netherlands). Library construction was performed using the TruSeq Stranded Total RNA LT Sample Prep Kit (Plant) with RiboZero and paired-end reads of 101 nt generated using the Illumina NovaSeq Platform. The quality of raw reads was assessed with FastQC (Andrews, 2010), adapter trimming was performed with fastp (Chen et al., 2018) (using the following settings: -q 20 --length_required 21 --cut_tail --cut_front --cut_mean_quality 20) and any ribosomal RNA (rRNA) was removed with BBDuk (https://sourceforge.net/projects/bbmap/) using the default settings (with the rRNA reference file ribokmers.fa) (Bushnell, n.d.). Host sequences were removed by aligning with the cucumber reference genomic sequence (GCF_000004075.3_Cucumber_9930_V3_genomic.fna) using BBSplit and the remaining reads were then de novo assembled using SPAdes (Bushnell, n.d.; Prjibelski et al., 2020) with the -meta option. Assembled contigs larger than 200 nt were subjected to BLASTn analysis using NCBI Blast+v2.9.0 (Camacho et al., 2009) against the RVDB database v20.0 (Goodacre et al., 2018). Taxonomic information relevant to results of interest was subsequently added using taxonomizr (https://cran.r-project.org/web/packages/taxonomizr/index.html).

2.2 | RT-PCR and Sanger sequencing

Complementary DNA (cDNA) synthesis was carried out with M-MuLV reverse transcriptase (Minotech Biotechnology, Greece) using 500 ng of total RNA and random hexamers, as per the manufacturer's instructions. The cDNA was diluted 1:5 in nuclease-free water and PCR was carried out using Taq DNA polymerase (Minotech Biotechnology, Greece) together with virus-specific primers according to manufacturer's instructions (Table S1). PCR amplicons were visualised by agarose gel electrophoresis and stained with ethidium bromide. Amplicons were excised and gel-purified using NucleoSpin® Gel and PCR Clean-Up columns (Macherey-Nagel, Germany) before direct Sanger sequencing was carried out by GENEWIZ (Leipzig, Germany).

To amplify and sequence the complete genomes of putative novel viruses, a suite of primers was designed using the HTS sequence data (Table S1). Fragments overlapping by at least 100 nt were amplified by PCR using Phusion® High-Fidelity DNA Polymerase (New England Biolabs, UK) according to the manufacturer's recommendations, using cDNAs generated with random hexamers as described previously.

2.3 | 5′ and 3′ RACE

For the 5′ and 3′ RACE PCR, the adapted protocol described previously (Scotto–Lavino et al., 2006a, 2006b), was followed using the SuperScript™ III One-Step RT-PCR System (Invitrogen, USA). Briefly, 5′-RACE used sequence-specific reverse primers (Table S1) to synthesise cDNA followed by a terminal deoxynucleotidyl transferase (ThermoFisher Scientific, USA) reaction, as per the manufacturer's recommendations. Single and/or nested PCR was then carried out using either Taq DNA polymerase (Minotech Biotechnology, Greece) or Phusion® High-Fidelity DNA Polymerase (New England Biolabs, UK). For 3′-RACE, oligo-dT was used for the cDNA synthesis, and then combined with sequence-specific forward primers (Table S1) for PCR. The final PCR products were excised, purified and analysed by Sanger sequencing as described previously.

2.4 | Sequence analyses

Sanger-derived sequences were trimmed and assembled using the ContigExpress package from VectorNTI Suite v11. Open reading frames (ORFs) were predicted and annotated using VectorNTI and the NCBI ORFfinder tool (NCBI, https://www.ncbi.nlm.nih.gov/orffinder/). Processed Sanger and HTS data were compared to sequences on the NCBI database using BLAST algorithms available on the NCBI website (http://blast.ncbi.nlm.nih.gov/Blast.cgi). Conserved protein domains were identified using NCBI (https://www.ncbi.nlm.nih.gov/Structure/cdd/wrpsb.cgi) (Lu et al., 2020) and by comparison with published sequences. For ZYFV, putative potyviral polyprotein cleavage sites were identified by comparison with other PRSV-subgroup members as described (Adams et al., 2005; Goh & Hahn, 2021), while P3N-PIPO was annotated as described by Chung et al. (Chung et al., 2008). For the new nepovirus, ORFinder was used for the detection of the polyproteins in both RNAs, with putative cleavage sites determined according to Safançon (Sanfaçon, 2022). Sequence alignments were carried out using MUSCLE in MEGA X (Kumar et al., 2018) and trees were generated using the Maximum-Likelihood method, with bootstrapping (1000 replicates) (Saitoul & Nei, 1987; Felsenstein, 1985). The evolutionary distances were computed using the JTT + G model as predicted by MEGA according to Hall (2013). RDP4 was used to identify possible recombination between the sequences identified in this study and published sequences (Martin et al., 2015).

2.5 | Mechanical inoculation and electron microscopy

Mechanical inoculation was performed as described previously (Katsarou et al., 2018). Briefly, 100 μg of frozen leaf tissue was homogenised in 1 mL of 50 mM sodium phosphate buffer pH 7.2. Two young leaves each from four 4-week-old *Nicotiana benthamiana* plants were dusted lightly with carborundum (Prolabo, VWR, Radnor, USA) and mechanically inoculated with 15 μL of the homogenised mixture. Plants were monitored for 7 days post-inoculation and leaf tissue was collected from new leaves for further analysis.

For TEM, *N. benthamiana* leaves were cut into small pieces of 1–2 mm and immediately fixed overnight at 4°C in 2.5% glutaraldehyde. Samples were then rinsed twice with 0.1 M, sodium cacodylate buffer (SCB) pH 7.2 for 15 min at 4°C, fixed with 1% osmium tetroxide (2 h, 4°C) and rinsed with SCB buffer three times for 15 min each at 4°C. Samples were dehydrated in ethanol solutions (30%, 50%, 70%, 80%, 90%, 95% and 100%) for 15 min each at 4°C and a final treatment with 100% ethanol for 20 min at room temperature. After immersion

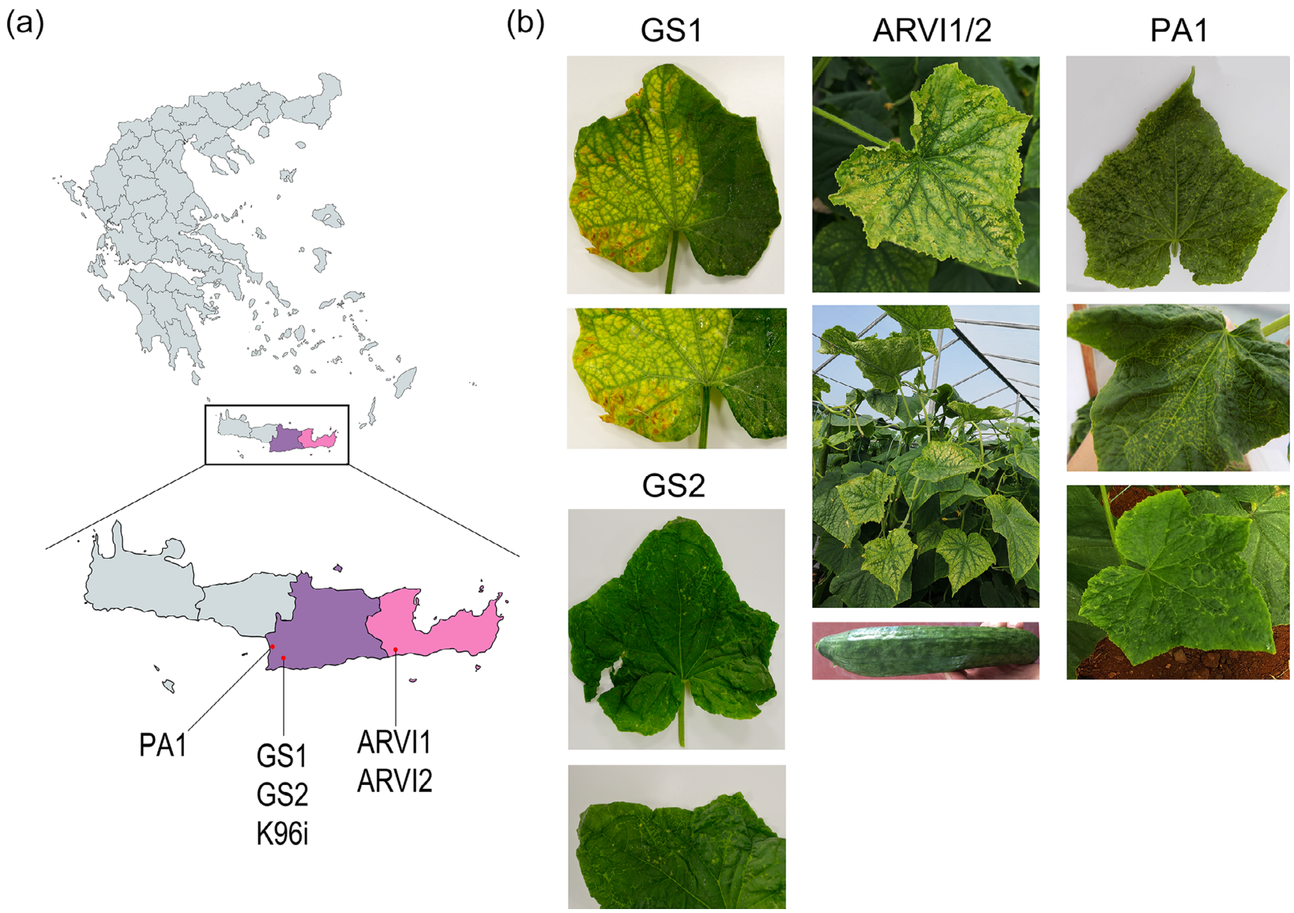

FIGURE 1 Samples used in this study. (a) Map showing cucumber collection sites in the regions of Heraklion (purple) and Lasithi (pink) on the island of Crete; and (b) Photographs depicting the observed symptoms in cucumber samples GS1, GS2, ARVI1, ARVI2 and PA1 used in this study.

in propylene oxide for 20 min (twice), samples were treated with a mixture of solutions made of resin embedding media (containing Durcupan single components A [M epoxy resin], B [hardener 964], C [accelerator 960] and D [plasticizer] in the ratio 10:10:0.3:0.3) mixed with propylene oxide at varying concentrations (V:V = 1:3 for 1 h, 1:1 for 1 h and V:V = 3:1 for 1 h), and finally with 100% resin embedding media overnight. Finally, samples were heated at 60°C for 48 h. Sections were cut on an Ultra microtome LEICA EM UC7 at a thickness of 70 nm. Sections were placed in glass slides and 2% methylene blue was applied for 5 min followed by a 5 min wash with distilled water. Slides were observed in a Nikon Eclipse E400 light microscope. Sections were placed on copper 200 mesh grids and stained with 0.2% lead citrate/7% uranyl acetate. Observations were made at 80 kV in a JEOL JEM-2100 electron microscope. At least 10 images of each organelle were taken to investigate a potential phenotype.

2.6 | Software

The map of Figure 1 was made using mapchart (https://www.mapchart.net), and Photoshop CS6 was used for image composition. SDTv1.2 was used for virus demarcation (http://web.cbio.uct.ac.za/~brejnev/) (Muhire et al., 2014).

TABLE 1 Details of the six cucumber field samples subjected to HTS for virus identification.

Sample name	Collection location in Crete	Symptoms
GS1	Messara	Chlorosis with necrotic areas
GS2	Messara	Chlorotic spots in the leaf and crinkling
ARVI1	Ierapetra	Severe chlorosis
ARVI2	Ierapetra	Severe chlorosis
PA1	Tympaki	Chlorotic regions mostly around the veins, yellow ringspots
K96i	Messara	Not recorded

3 | RESULTS

3.1 | Next-generation sequencing and virus identification

In 2019, routine pathology sampling of vegetable crops in Crete included samples of cucumbers collected from several locations. Six samples from Messara, Ierapetra and Tympaki regions (Table 1, Figure 1a) showed symptoms characteristic of virus infection, including chlorotic patterns or spots, mosaic, severe yellowing, necrosis,

TABLE 2 Large contigs from de novo assembly with high identity to known plant viruses.

Contig	Length (nt)	Identity based on BLASTn analysis	GenBank accession for comparison	% nt similarity (BLASTn)	Putative full-length sequence?
NODE_1	10,403	Papaya ringspot virus	KC345609.1	96	Yes
NODE_2	10,367	Papaya ringspot virus/zucchini yellow fleck virus	MH444652.1/ NC_043173	68/87	Yes
NODE_4	9135	Cucurbit yellow stunting disorder virus RNA1	NC_004809.1	99.2	Yes
NODE_5	8554	Cucurbit chlorotic yellows virus RNA 1	NC_018173.1	99.8	Yes
NODE_6	8048	Cucurbit chlorotic yellows virus RNA 2	NC_018174.1	99.8	Yes
NODE_7	8007	Cucurbit yellow stunting disorder virus RNA2	NC_004810.1	99.6	Yes
NODE_8	7129	Artichoke Italian latent virus RNA 1	NC_043684.1	80.4	Yes
NODE_10	6551	Artichoke Italian latent virus RNA 1	NC_043684.1	80.7	Yes
NODE_11	4861	Cucurbit aphid-borne yellows virus	NC_003688.1	95.8	No (approx. 86%)
NODE_13	4480	Artichoke Italian latent virus RNA 2	NC_043685.1	74.2	Yes

ringspots, vein yellowing and/or leaf crinkling (Figure 1b) were selected for HTS to identify any viruses present.

350 ng of purified RNA from each of the six samples was pooled and subjected to HTS using the Illumina NovaSeq Platform, with a total of 57,828,340 raw reads obtained. Following de novo assembly and BLAST analysis, several large contigs with high identity to known plant viruses were identified (Table 2). These included two contigs with high identity to PRSV and ZYFV, two contigs with high identity to CYSDV (with one contig each representing genomic RNAs 1 and 2), two contigs with high identity to CCYV (with one contig each representing genomic RNAs 1 and 2), three contigs with high identity to the nepovirus artichoke Italian latent virus (AILV), with two contigs representing RNA1 and one contig representing RNA2; and one contig with high identity to CABYV. Out of the 10 large contigs assembled, nine represented near full-length sequences of the corresponding genomic RNAs to which they matched (Table 2). The only exception was for Node_11, where the ~4.8 kb contig showed 85.7% coverage of the most similar published sequence (GenBank accession no. X76931), corresponding to genomic positions 11 to 4867 of CABYV. For the three contigs with similarity to AILV (Node_8, Node_10 and Node_13), the two contigs representing RNA1 showed only ~80% similarity with published sequences, while RNA2 showed 74.2% similarity across 62% of the contig (5′ region), and no significant similarity to the 3′ end was identified using BLASTn. When BLASTx was used, the 3′ region showed only ~35% amino acid identity with coat protein sequences for several members of the genus *Nepovirus*, suggesting these contigs may represent a novel virus sequence. The two RNA1 sequences shared 86.4% nt identity suggesting they were isolates of the same virus. Node_2 showed only 68% nt identity with PRSV across the complete sequence; however, the 3′ end showed high identity (87%) with several partial ZYFV sequences.

In addition to the 10 large contigs, a number of smaller contigs with high identity to plant viruses were also identified. Two contigs, both with a length of 749 nt, also showed high similarity (92.8% and 89.8%, respectively) to CABYV. Comparison of these two contigs with published sequences showed that they both map to the same position at the 3′ end of the viral genome and would complement the large contig from NODE_11 described earlier. Finally, 20 contigs ranging from 209 to 2170 nt with 80 to 100% nt identity to PRSV suggested the presence of at least one additional sample with this virus, while 18 contigs (varying in length from 211 to 788 nt) with at least 93.8% identity to cucurbit cytorhabdovirus 1 (CuCV1, genus *Cytorhabdovirus*) suggested the presence of this virus in at least one sample. The presence of all these contigs was indicative of one or more samples infected with potyvirus (either PRSV or ZYFV) as well as a putative novel nepovirus, while at least one sample was infected with CABYV, CCYV, CuCV1 and CYSDV.

3.2 | RT-PCR and Sanger sequencing to confirm virus infections

To confirm the presence of each virus and identify which plant samples were infected, the RNA extracted from the six samples was individually subjected to RT-PCR with a suite of virus-specific primers (Table S1). PCR screening identified CYSDV in sample GS1, CuCV1 and ZYFV in sample GS2, PRSV in samples ARVI1 and ARVI2, CCYV in sample PA1, and CuCV1, CCYV, together with CABYV in sample K96i (Figure 2). In addition, primers designed using the NODE_8 and NODE_13 contigs with similarity to AILV resulted in four samples testing positive (Figure 2). Direct sequencing of the PCR amplicons confirmed the identity of each virus in the samples.

The presence of one large contig (NODE_11) representing 85% of the complete CABYV genome from the 5′ end, together with two smaller contigs (NODE_444 and NODE_445), representing the remaining 3′ end of the virus, suggested at least two virus isolates were present for CABYV (Table 2). However, only a single sample

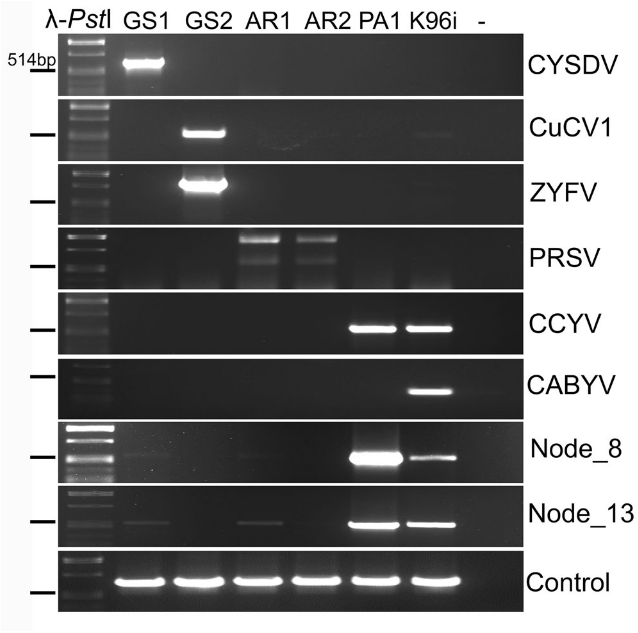

FIGURE 2 PCR analysis to confirm the presence of viruses identified following high-throughput sequencing of RNA from cucumber samples collected in Crete. Screening PCRs were conducted for cucurbit yellow stunting disorder virus (CYSDV), cucurbit cytorhabdovirus 1 (CuCV1), zucchini yellow fleck virus (ZYFV), papaya ringspot virus (PRSV), cucurbit chlorotic yellows virus (CCYV), cucurbit aphid-borne yellows virus (CABYV), the novel nepovirus with primers targeting RNA1 (Node_8) or RNA2 (Node_13). Elongation factor 1 (Control) was used as a positive control to confirm successful cDNA synthesis. DNA size marker is λ-phage DNA digested using *Pst*I. Bar represents a fragment of 514 bp. Samples are GS1, GS2, ARVI1 (AR1), ARVI2 (AR2), PA1 and K96i. – denotes the no template control for each PCR set.

tested positive by RT-PCR (K96i). To resolve the possibility that sample K96i contained two distinct sequences, a second set of screening primers was designed, with a single forward primer (CAVBYV_3′fwd; Table S1) designed at a position where the two sequences were identical, together with two reverse primers (CABYV_444R and CABYV_445R; Table S1) designed at a position where the sequence varied between the two contigs. Further RT-PCR screening using these primers, followed by Sanger sequencing of the amplicons, confirmed that two distinct sequence variants were present in sample K96i (Figure S1).

Analysis of the contigs assembled following HTS identified three contigs with similarity to the nepovirus AILV, including two contigs corresponding to RNA1 (NODE_8 and NODE_10), and one contig corresponding to RNA2 (NODE_13; Table 2). Comparison of the two RNA1 sequences showed they share 86.4% identity at the nucleotide level, with NODE_8 covering approximately 95% of the AILV reference sequence, while NODE_10 was 578 nt shorter than NODE_8 and covered approximately 87% of the AILV reference sequence. To determine which of the samples were infected with the novel nepovirus, primers were designed for both RNA1 (NODE_8_Fw/NODE_8_10_R) and RNA2 (NODE_13_F_F /NODE_13_CP_R) and used in PCR, with four samples testing positive (Figure 2).

As the HTS analysis identified a putative novel nepovirus sequence from cucumbers in Crete, and no complete genome sequence was available for ZYFV at the time of the study, the complete genomes of these two viruses were fully characterised.

3.3 | Complete genome sequencing of zucchini yellow fleck virus

To confirm the complete genome sequence of the ZYFV isolate identified in the HTS analysis, RT-PCR and Sanger sequencing was carried out using a series of overlapping primers (Table S1) designed using the NODE_2 sequence from the HTS assembly. Direct sequencing of the PCR products (Figure S2) confirmed approximately 9.5 kb of the sequence from the HTS assembly. The 5′ and 3′ ends of the genomic sequence were subsequently confirmed using 5′ and 3′ RACE, respectively. The complete genome sequence compiled from the Sanger sequencing was aligned to the NODE_2 sequence for comparison and four nt (CCCC) at the 5′ end of the HTS-generated contig were removed to match sequence reads from the 5′ RACE. All other nt positions of the Sanger sequences were identical to the HTS assembly. The complete genome sequence was submitted to GenBank under accession number PP376099.

The complete genome sequence of the ZYFV genome comprised 10,338 nt excluding the polyA tail. Sequence analysis confirmed the presence of a large polyprotein-encoding ORF, typical of potyviruses, of 10,008 nt, encoding a protein of 3335 aa. BLASTn analysis of the complete genome revealed 79.18–84.16% nt identity with seven recently published ZYFV isolates from Greece and Italy (ON456303-ON456309), as well as 81.92 to 87.21% identity with several partial sequences (of the CP-coding region) from Italy and France. BLASTp analysis of the complete polyprotein aa sequence showed 84 to 92.5% sequence similarity with the ZYFV isolates, followed by 63.96% identity with Zucchini tigre mosaic virus (ZTMV) and 62.9% to PRSV. Comparison using the CP aa sequence confirmed 87.9–96.2% identity with the published ZYFV isolates. In addition to the polyprotein-encoding ORF, a small 241 nt ORF P3N-PIPO potentially encoding a protein of 79 aa was also identified, which was associated with the characteristic $G_{1\text{-}2}A_{6\text{-}7}$ sequence motif present within the P3 coding region. BLASTp analysis of the translated aa sequence of this small ORF revealed approximately 76.9–93.6% aa identity with ZYFV PIPO aa sequences, with the next most similar sequence from PRSV with 56.9% similarity. In addition to the two ORFs, the complete genome sequence had a 5′ UTR of 120 nt and a 3′ UTR of 210 nt. Comparison of the 5′ end of the viral genomic sequence confirmed a stretch of 27 nt (AAAAUAAAACAACUCAACACAACACAA) which are highly conserved among ZYFV and other members of the PRSV subgroup, including PRSV and ZTMV.

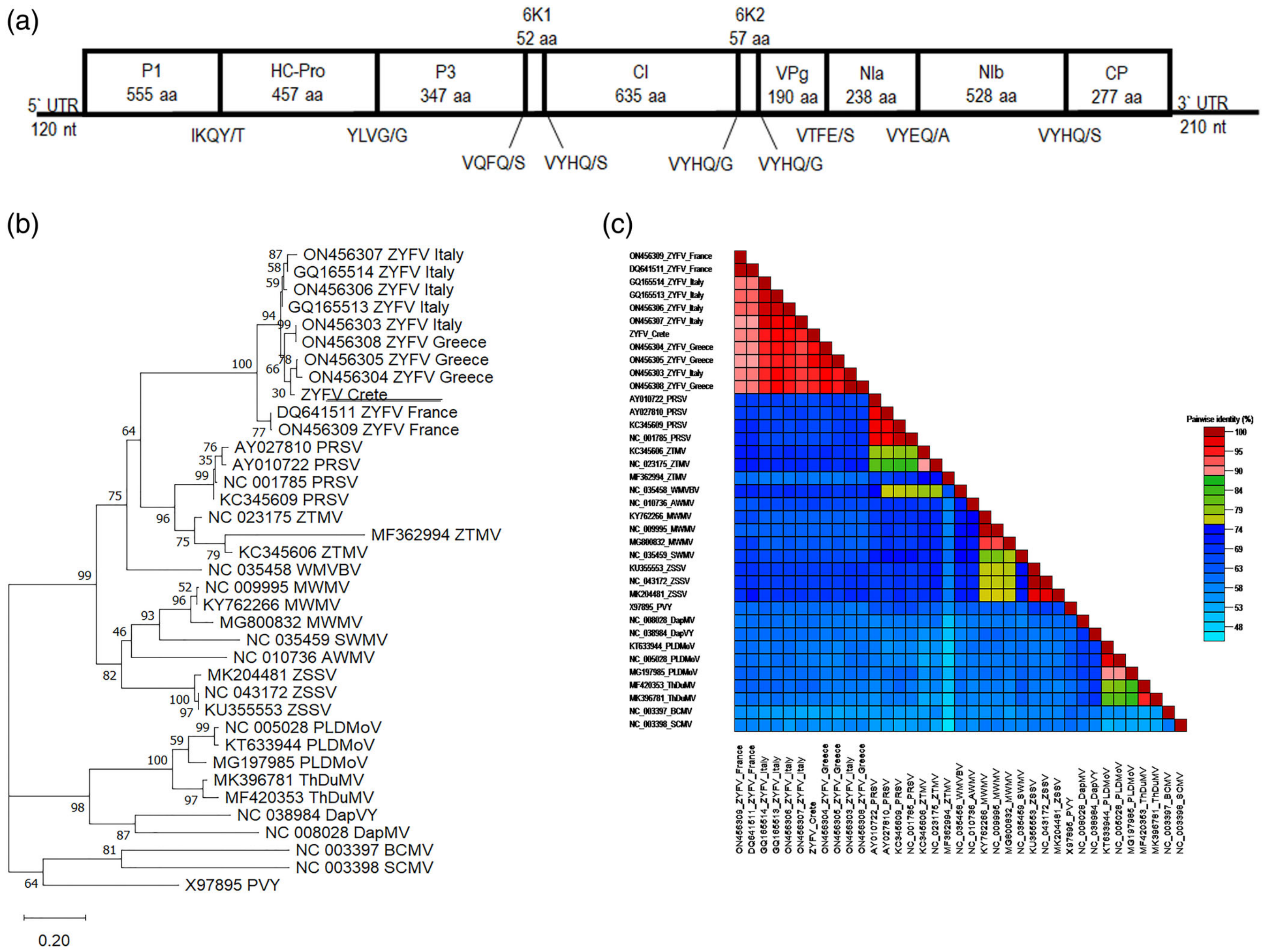

FIGURE 3 Characterisation of zucchini yellow fleck virus (ZYFV) from cucumber in Crete. (a) Schematic representation of the complete genome of ZYFV from Crete including putative cleavage sites of the virus-encoded proteases to generate the 10 mature peptides P1, HC-Pro, P3, 6 K1, CI, 6 K2, VPg, NIa, NIb and CP. UTR – untranslated region; (b) Phylogenetic analysis of ZYFV from Crete together with other ZYFV isolates and members of genus *Potyvirus*. Published sequences of ZYFV from France, Greece and Italy were aligned together with the isolate from Crete and selected isolates of Algerian watermelon mosaic virus (AWMV), Daphne mosaic virus (DapMV), Moroccan watermelon mosaic virus (MWMV), papaya leaf distortion mosaic virus (PLDMoV), papaya ringspot virus (PRSV), Sudan watermelon mosaic virus (SWMV), Thladiantha dubia mosaic virus (ThDuMV), watermelon vein banding virus (WMVBV), zucchini shoestring virus (ZSSV) and zucchini tigre mosaic virus (ZTMV). Potato virus Y (PVY), bean common mosaic virus (BCMV) and sugarcane mosaic virus (SCMV) were used as outgroups. Reference numbers of the accessions used are listed in Table S4. Alignment of trimmed coat protein amino acid sequences was carried out in MEGA X using MUSCLE, with trees generated using the Maximum-Likelihood method (JTT + G) model and 1000 bootstrap replications; and C) Analysis of ZYFV from Crete together with other ZYFV isolates and members of genus *Potyvirus* using SDTv1.2 (Muhire et al., 2014).

The putative polyprotein cleavage sites were identified following analysis of the complete polyprotein aa sequence of ZYFV and comparison with other members of the PRSV-subgroup (Figure 3a, Table S2). Consistent with previous reports, two putative cleavage sites were identified near the NIb-CP junction, while the DAG aa motif at the 5′ end of the CP was confirmed as DAA in this isolate and is consistent with other full-length ZYFV isolates.

Phylogenetic analysis of the trimmed CP aa sequence of ZYFV from Crete, together with other members of the PRSV subgroup (Table S4), confirmed the close relationship of this isolate with other ZYFV isolates previously sequenced from Greece and Italy, as well as their close relationship with isolates of PRSV and ZTMV (Figure 3b). Similarly, using SDT the high sequence similarity of the known ZYFV isolates from Greece, including the Cretan isolate sequenced herein, together with isolates from Italy, confirmed they are members of a single species group (Figure 3c).

3.4 | Complete genome sequencing of a novel nepovirus from cucumber

As with ZYFV, a series of overlapping primers were designed using the three nepovirus-like contigs (Table S1) and were used in PCRs to amplify the complete genome from sample PA1 (Figure S3).

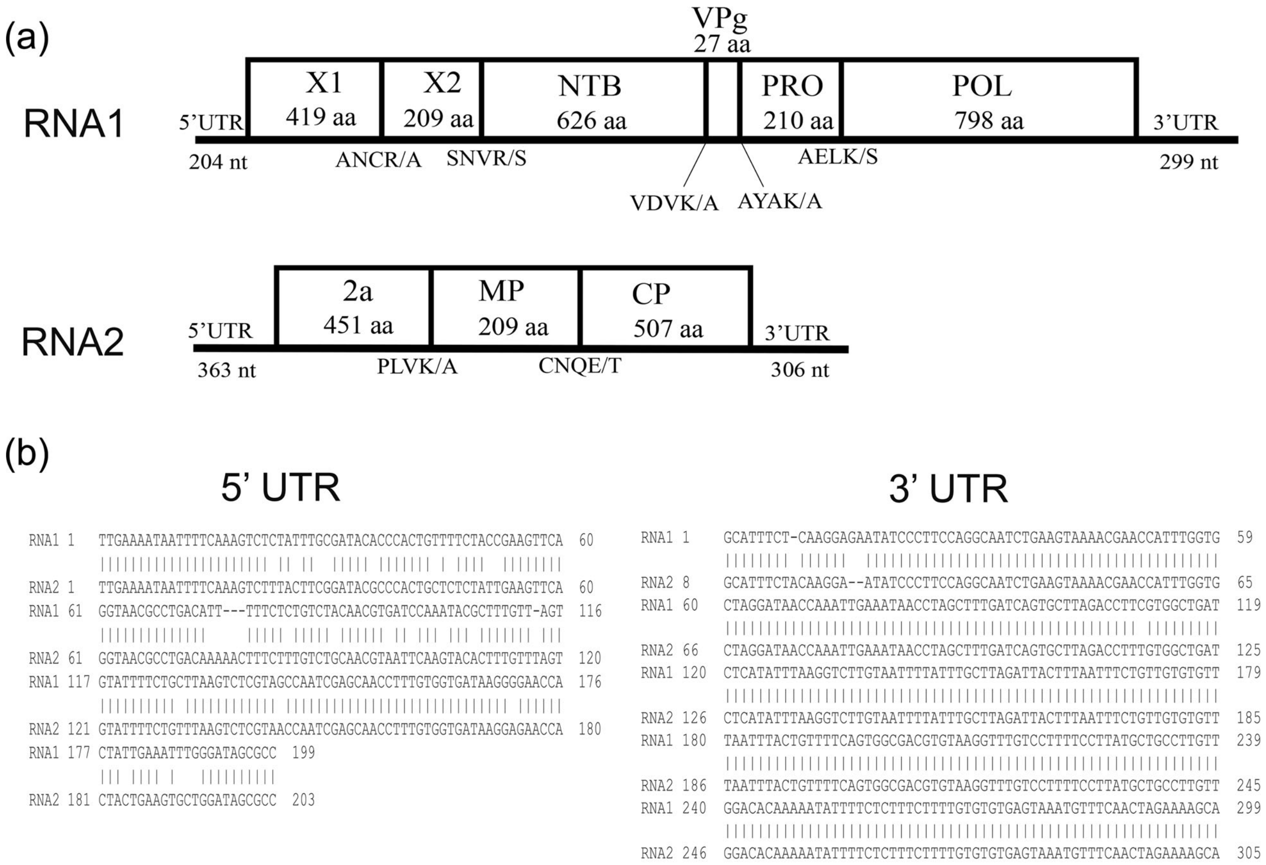

```
RNA1 1   TTGAAAATAATTTTCAAAGTCTCTATTTGCGATACACCCACTGTTTTCTACCGAAGTTCA  60
         |||||||||||||||||||||| || ||  ||||| ||||||| | ||||  ||||||||
RNA2 1   TTGAAAATAATTTTCAAAGTCTTTACTTCGGATACGCCCACTGCTCTCTATTGAAGTTCA  60
RNA1 61  GGTAACGCCTGACATT---TTTCTCTGTCTACAACGTGATCCAAATACGCTTTGTT-AGT  116
         ||||||||||||||     ||||| ||||| |||||| || ||| ||| ||||||| |||
RNA2 61  GGTAACGCCTGACAAAAACTTTCTTTGTCTGCAACGTAATTCAAGTACACTTTGTTTAGT  120
RNA1 117 GTATTTTCTGCTTAAGTCTCGTAGCCAATCGAGCAACCTTTGTGGTGATAAGGGGAACCA  176
         |||||||||| |||||||||||| ||||||||||||||||||||||||||||| ||||||
RNA2 121 GTATTTTCTGTTTAAGTCTCGTAACCAATCGAGCAACCTTTGTGGTGATAAGGAGAACCA  180
RNA1 177 CTATTGAAATTTGGGATAGCGCC  199
         ||| |||| |   ||||||||||
RNA2 181 CTACTGAAGTGCTGGATAGCGCC  203
```

```
RNA1 1    GCATTTCT-CAAGGAGAATATCCCTTCCAGGCAATCTGAAGTAAAACGAACCATTTGGTG  59
          |||||||| ||||||  |||||||||||||||||||||||||||||||||||||||||||
RNA2 8    GCATTTCTACAAGGA--ATATCCCTTCCAGGCAATCTGAAGTAAAACGAACCATTTGGTG  65
RNA1 60   CTAGGATAACCAAATTGAAATAACCTAGCTTTGATCAGTGCTTAGACCTTCGTGGCTGAT  119
          |||||||||||||||||||||||||||||||||||||||||||||||||| |||||||||
RNA2 66   CTAGGATAACCAAATTGAAATAACCTAGCTTTGATCAGTGCTTAGACCTTTGTGGCTGAT  125
RNA1 120  CTCATATTTAAGGTCTTGTAATTTTATTTGCTTAGATTACTTTAATTTCTGTTGTGTGTT  179
          ||||||||||||||||||||||||||||||||||||||||||||||||||||||||||||
RNA2 126  CTCATATTTAAGGTCTTGTAATTTTATTTGCTTAGATTACTTTAATTTCTGTTGTGTGTT  185
RNA1 180  TAATTTACTGTTTTCAGTGGCGACGTGTAAGGTTTGTCCTTTTCCTTATGCTGCCTTGTT  239
          ||||||||||||||||||||||||||||||||||||||||||||||||||||||||||||
RNA2 186  TAATTTACTGTTTTCAGTGGCGACGTGTAAGGTTTGTCCTTTTCCTTATGCTGCCTTGTT  245
RNA1 240  GGACACAAAAATATTTCTCTTTCTTTTGTGTGTGAGTAAATGTTTCAACTAGAAAAGCA  299
          ||||||||||||||||||||||||||||||||||||||||||||||||||||||||||||
RNA2 246  GGACACAAAAATATTTCTCTTTCTTTTGTGTGTGAGTAAATGTTTCAACTAGAAAAGCA  305
```

FIGURE 4 Characterisation of a novel nepovirus from cucumber in Crete. (a) Schematic representation of the genome organisation of RNA1 and RNA2 of the novel nepovirus identified in this study. RNA1 encodes a polyprotein cleaved into the X1, X2, NTB, VPg, PRO and POL proteins, while RNA2 is cleaved into the 2a, MP and CP proteins; (b) Nucleotide sequence alignment of the 5′ and 3′ UTRs of RNA1 and RNA2 showing regions with high similarity between the two genome components of the novel virus sequence.

Comparison of the Sanger sequencing results for RNA1 and RNA2 with the HTS contigs showed that the PCR-amplified fragments from sample PA1 were identical to NODE_8 and NODE_13. The 5′ and 3′ ends of the two genomic RNAs were then obtained using 5′ and 3′ RACE. RNA1 comprised 7370 nt including the 5′ and 3′ UTRs, while the complete sequence of RNA2 was 4707 nt including the 5′ and 3′ UTRs (Figure 4a). The complete sequences of RNA1 and RNA2 for the novel virus from sample PA1 were deposited in GenBank under accession numbers PP376097 and PP376098, respectively.

Analysis of the complete genome sequence of RNA1 identified a single ORF of 6867 nt, encoding a putative polyprotein of 2288 aa with a predicted molecular mass (M_r) of 256 kDa, with a 5′ UTR of 204 nt and a 3′ UTR of 299 nt (Figure 4a). BLASTp of the translated ORF sequence revealed 87.1% aa identity with AILV, followed by ~81% identity with several isolates of beet ringspot virus (BRSV). Alignment of the complete sequence of RNA1 with the published AILV RNA1 sequence confirmed 79.6% nt identity between the two complete sequences. The next most similar sequences were isolates of BRSV, with ~74% nt identity across the complete RNA1. Similarly, RNA2 also possessed a single ORF of 4038 nt, predicted to encode a polyprotein of 1345 aa (M_r 149 kDa) with a 5′ UTR of 363 nt and a 3′ UTR of 306 nt. For RNA2, the complete sequence showed 64.6% nt identity with the AILV RNA2 and ~ 62% nt identity with isolates of BRSV and tomato black ring virus (TBRV). As is typical of members of the family *Secoviridae*, a high level of nt similarity was identified between the 5′ and 3′ UTRs of RNA1 and RNA2, including 99% similarity between the 3′ UTRs (Figure 4b).

To investigate the putative cleavage sites within the polyproteins encoded by RNA1 and RNA2, the translated amino acid sequences of the novel nepovirus were aligned together with published polyprotein sequences for other members of the genus (Table S3 and Figure S4). Based on the alignment of RNA1 (Figure S4), the putative cleavage site between the X1 and X2 proteins was determined as 'RA' at aa position 419 (1461 nt). The cleavage between X2 and NTB was predicted to be 'RS' at aa position 628 (2088 nt), whereas the NTB-VPg cleavage site was predicted to be 'KA' at position 1227 (3885 nt). The cleavage site between the VPg and 3CL-PRO proteins was predicted as 'KA' at position 1254 (3966 nt) while the possible cleavage site between 3CL-PRO and POL was predicted to be 'KS' at aa 1464 (4596 nt) (Figures 4a and S4). Based on the identified cleavage sites,

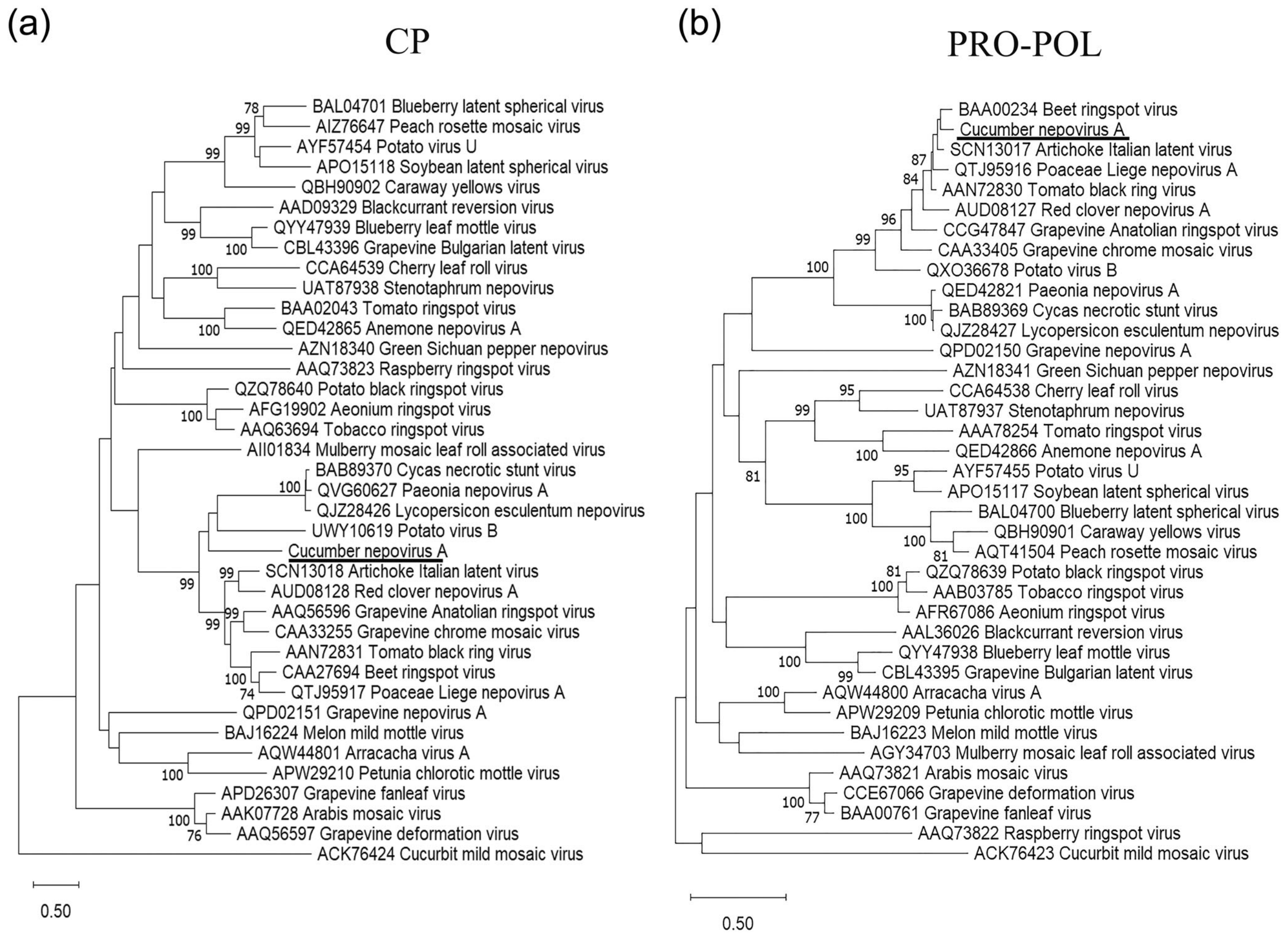

FIGURE 5 Phylogenetic analysis of RNA1 and RNA2 of the novel nepovirus identified in this study. (a, b) Phylogenetic analysis of the CP or PRO-POL protein sequences, together with reference sequences of other published nepoviruses (Table S4). Alignment of trimmed amino acid sequences was carried out in MEGA X using MUSCLE, with trees generated using the Maximum-Likelihood method (JTT + G) model and 1000 bootstrap replications.

M_r of each of the mature proteins was predicted to be 48 kDa (X1), 23 kDa (X2), 66 kDa (NTB), 3.1 kDa (VPg), 23 kDa (3CL-PRO) and 92 kDa (POL). For 3CL-PRO the 'catalytic triad' that defines the active site of this enzyme was identified as histidine at position 1294, glutamic acid at position 1330 and cysteine at position 1424.

Using the same approach, the RNA2 polyprotein was analysed for putative cleavage sites. However, since RNA2 significantly differs between the different subgroups of nepoviruses, alignments were only done using members of subgroup B, which are most similar to the novel sequence (Figures 5a and S4). Typically, three proteins are produced from the cleavage of the polyprotein encoded by the ORF of RNA2. A cleavage site between the 2a and MP proteins was predicted at an atypical aa motif for the group of 'KA' at position 451 in the protein sequence (1716 nt), producing a 2a protein of 50 kDa. The second cleavage site was more difficult to identify based on the aa alignment since again an atypical 'ET' cleavage site was indicated at position 839 (2880 nt); however, a more typical 'MA' site found five aa upstream of this position is also possible based on comparison with melon mild mottle virus (MMMoV), a nepovirus of subgroup A. Based on these cleavage sites the MP is predicted to have a M_r of ~43 kDa, while the CP is predicted to have a M_r of ~56 kDa (Figures 4a and S4).

To determine the phylogenetic relationship of the novel nepovirus sequence with other members of the genus *Nepovirus*, pairwise sequence comparison and phylogenetic analysis were performed (Figures 5 and S5 and Tables S5 and S6). According to the ICTV, distinct species in the genus *Nepovirus* share less than 75% aa sequence similarity within the CP region and/or less than 80% aa sequence similarity within the PRO-POL region (the region between the 'CG' motif of 3CL-PRO and the 'GDD' motif of POL), as well as differences in host plant species and vector transmission. Analysis of sequence similarity between the CP region of this virus and other members of the genus *Nepovirus* identified only 19%–38% aa sequence similarity, with the highest similarity to red clover nepovirus A (Figure S5a, Table S5). In contrast, a comparison of the PRO-POL aa sequence identified 89–91% similarity to isolates of BRSV and AILV (Figure S5b, Table S6).

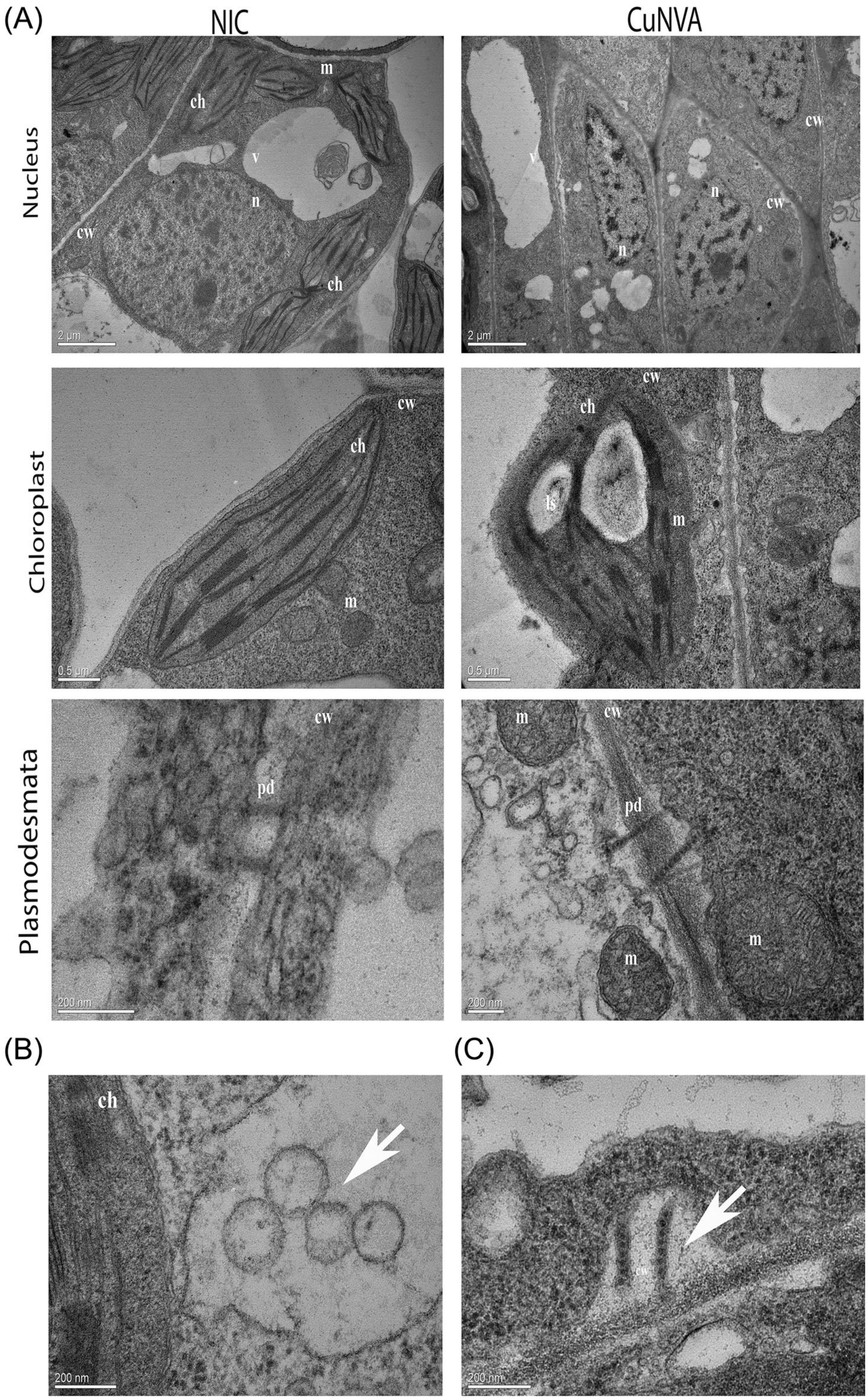

FIGURE 6 Cytopathological changes induced in *Nicotiana benthamiana* plants mechanically inoculated with the novel nepovirus. (a) Representative TEM cross-sections of non-inoculated control plant (NIC) and CuNVA-inoculated plant showing representative nucleus, chloroplast and plasmodesmata structures; (b) Cross-section of inoculated plant representing possible viral factories, the potential site of viral replication (arrow); C) TEM cross-section from inoculated plant showing tubular structures with virus-like particles in close proximity to plasmodesmata. 'ch' – chloroplast, 'n' -nucleus, 'v' – vacuole, 'cw' – cell wall, 'm' – mitochondria and 'pd' – plasmodesmata.

Phylogenetic analysis using PRO-POL regions also confirmed that the novel virus is most closely related to BRSV and AILV in nepovirus subgroup C. However, analysis using the CP region showed that the novel virus is most closely related to viruses of nepovirus subgroup B (Figure 5a,b). Recombination analysis using RDP4, based on published complete genome sequences for both RNA1 (119 sequences) and RNA2 (101 sequences) of all currently accepted members of the genus could identify no clear recombination signals between this new virus and other previously characterised nepoviruses (Figure S6, Table S7).

Finally, electron microscopy was carried out to investigate any cytopathological effects resulting from infection of the novel nepovirus in *N. benthamiana*. One-week post-inoculation plants showed a faint yellowing in newly developed leaves, followed by a recovery phenotype observed approximately 10 days post-inoculation. RT-PCR (using primers NODE_8_Fw/NODE_8_10_R, NODE_13_F_F/NODE_13_CP_R) followed by Sanger sequencing, confirmed the infection of *N. benthamiana* plants with the nepovirus (Figure S7a). Using light microscopy no obvious disruption of the leaf structure was noted, supporting the mild nature of this virus infection in *N. benthamiana* (Figure S7b). When transmission electron microscopy (TEM) was used to assess the effects of virus infection on plant organelle structure, no effects were observed on the nuclei of cells from infected leaf tissue, whereas chloroplasts showed a mild swelling combined with the presence of large starch granules (Figure 6a). In addition, we observed membranous round structures in the cytoplasm which could correspond to viral factories (Figure 6b). The most characteristic observation was the presence of tubular structures, containing smaller, isometric structures (possibly representing virus particles) identified in or close to plasmodesmata (Figure 6c).

The ICTV recommends additional criteria to be considered when proposing a novel virus in the family *Secoviridae* when high sequence similarity is observed in either the Pro-Pol or CP region. However, based on the low level of sequence identity in the CP region compared with other nepoviruses, the lack of any recombination with other viruses detected in our analysis and the occurrence of this virus in cucumber, we propose this new virus sequence to be considered as a novel member of the genus *Nepovirus* and be named cucumber nepovirus A (CuNVA).

4 | DISCUSSION

In this study, we have collected cucumbers grown under greenhouse conditions from several regions of the island of Crete and characterised the viruses present using HTS followed by RT-PCR and Sanger sequencing. These cucumbers presented symptoms indicative of virus infection, including chlorotic patterns or spots, mosaic, severe yellowing, necrosis, ringspots, vein yellowing and/or leaf crinkling. Six samples were pooled for HTS with at least seven distinct viruses identified following analysis of the HTS data including several viruses already identified in Greece, including Crete, such as CABYV (Boubourakas et al., 2006), CCYV (Orfanidou et al., 2014), CuCV1 (Orfanidou et al., 2020), CYSDV (Orfanidou et al., 2019) and PRSV (Avgelis & Vovlas, 1986). The presence of these viruses was verified by RT-PCR and Sanger sequencing, and are summarised in Table 3. To our knowledge, this is the first record of CuCV1 infection described from cucumber. In addition, we identified a near complete genome sequence of ZYFV, a virus previously reported from France, Greece and Italy (Avgelis, 1985; Gilbert-Albertini & Lecoq, 1994; Vovlas et al., 1981) but with no complete genome published at the time of the study, and a potential novel nepovirus, provisionally named CuNVA.

ZYFV is one of eight members of the PRSV subgroup of the genus *Potyvirus* known to infect cucurbits, including several edible species such as melons, squash and cucumber as well as the non-edible plant squirting cucumber and model plants such as *N. benthamiana* and *Chenopodium amaranticolor* (Gilbert-Albertini & Lecoq, 1994). Symptoms of ZYFV vary from mosaic and leaf distortion, pin-point yellow spots or yellow flecks, to vein necrosis and lethal necrosis, with symptoms sometimes also present on the fruits of infected plants (Gilbert-Albertini & Lecoq, 1994; Tomassoli et al., 2010). Symptoms in the cucumber plant GS2 with ZYFV (in a mixed infection with CuCV1) showed mild mosaic and were far less severe when compared with ARVI1/2 having PRSV infection. This result suggests that in cucumber this isolate of ZYFV is not severe, although any effect must be considered with the knowledge that a mixed infection was observed. Until recently, only three partial sequences of ZYFV were published including isolates from France and Italy; however the complete genomes of six geographically diverse isolates were recently reported, including one from squash collected in Greece, four from zucchini collected from Italy and Greece, and one from *E. elaterium* from France (Sareli et al., 2022). The ZYFV isolate from cucumber sequenced here has high nucleotide (75.9–83.8%) and amino acid (83.9–92.5%) sequence identity with the six complete genomes previously published, with the isolate from France being the most dissimilar. Phylogenetic analysis confirmed that the sequence from Crete clusters with the other ZYFV members of the PRSV subgroup. However, unlike the Greek ZYFV isolate sequenced from squash, the isolate from cucumber did not possess the novel repeated NSSVEM motif identified in the P1 protein, while other motifs such as the DAA motif for aphid transmission and the repeated cleavage sites at the NIB-CP junction were consistent with all previous ZYFV full-length genome sequences (Sareli et al., 2022). This is the first full-length sequence of ZYFV from Crete and from the host cucumber.

TABLE 3 Viruses identified from cucumber leaf samples used in this study.

Sample	Viruses
GS1	GYSDV, CuNVA
GS2	CuCV1, ZYFV
ARVI1	PRSV, CuNVA
ARVI2	PRSV
PA1	CCYV, CuNVA
K96i	CCYV, CABYV, CuNVA

Additionally, in this study, we have identified a tentative novel member of the genus *Nepovirus*. Nepoviruses are bipartite RNA viruses, belonging to the family *Secoviridae*, capable of infecting a wide variety of plants including grapes, potatoes, tomatoes, olives and apricots, all widely cultivated on the island of Crete (Sanfaçon, 2008). To our knowledge, there are only two nepoviruses identified in cucumbers, namely TRSV (Desbiez, 2020; Moore & McGuire, 1968) and AYRSV (Avgelis & Vovlas, 1989), however, neither belongs to subgroup B of the genus. The novel sequence identified has high similarity (89–91%) to characterised viruses in the Pro-Pol region of RNA1, but low similarity (19–38%) in the CP region of RNA2. When sequence similarity is high, the ICTV indicates that other criteria, including host range, vector specificity and possibility of recombination should be considered. In our case, the very low sequence identity in the CP region and the absence of any recombination in RNA1 or 2, suggests that CuNVA may represent a new species in the genus *Nepovirus*. However, at this time information is not available on transmission of CuNVA by a vector.

The newly identified CuNVA, contains two RNAs of 7370 nt and 4707 nt. Comparison of these RNAs with characterised nepoviruses suggests this virus probably belongs to subgroup B within the genus *Nepovirus*, the first virus of this subgroup identified infecting cucumbers. Although CuNVA is most closely related to AILV and BRSV when comparing the PRO-POL encoding region of the genome, comparison with other nepoviruses using the CP-encoding region shows very low sequence similarity (∼19 to 38% aa identity) with all characterised nepoviruses. This observation is consistent with previous studies, for example, BRSV and TBRV, where 89% aa identity is observed within the RdRp region but only 62% aa identity in the CP protein (according to ICTV https://ictv.global/report/chapter/secoviridae/secoviridae and Hily et al. (2021)), however in the present case the similarity in the CP region is extremely low when compared with all other characterised members of the genus. Phylogenetic analysis using the CP region also showed CuNVA as most closely related to subgroup B, since the nearest sequence belongs to potato virus B. Recombination events have previously been identified in nepoviruses, including within RNA2 of AILV, a close relative of CuNVA, which was demonstrated to be a recombinant with BRSV and grapevine chrome mosaic virus (GCMV) (Fuchs et al., 2017; Hily et al., 2021). However, the present study failed to identify recombination between CuNVA and other nepoviruses characterised at this time.

When studying CuNVA RNAs, a high homology between their 5′ (86%) and 3′ (99%) UTRs was confirmed, as is common for all nepoviruses. Both CuNVA RNAs produce large polyproteins processed via the viral protein 3C-PRO. By comparison with other nepoviruses, we were able to identify the potential cleavage sites used by this protease. All cleavage sites of RNA1 were typical of viruses of this family as previously described (Sanfaçon, 2022). However, for the polyprotein encoded by RNA2, prediction of the cleavage sites was more complicated. An atypical ‘KA’ site was predicted between 2a-MP, as well as a possible ‘ET’ or ‘MA’ site (with ‘MA’ being 5 aa upstream of ‘ET’) for the MP-CP cleavage site. ‘ET’ is an aa combination that has not previously been identified in nepoviruses as a potential cleavage site from this viral protease, according to the analysis of characterised viral species, whereas an ‘MA’ cleavage site at this position has already been described before for MMMoV, suggesting this is the more plausible option (Sanfaçon, 2022).

Nepoviruses are transmitted by nematodes, mites, pollen and seeds as well as mechanically (Fuchs et al., 2017; Sanfaçon, 2008). Infected plants usually display chlorosis and ringspot symptoms, similar to those observed on the leaves from sample PA1 in the present study. However, this plant sample was also infected with CCYV. Therefore, no conclusions about the symptoms induced by infection with CuNVA in cucumber can be made at the present time. Mixed infections were also observed in three other samples (GS1, ARVI1 and K96i). Another characteristic of this family is the transient infection phenotype observed, due to the recovery effect, which can complicate diagnosis in infected plants. Using the cucumber leaf tissue of sample PA1, CuNVA was mechanically inoculated to *N. benthamiana* plants, with PCR and sequencing confirming that mechanical infection is an alternative transmission route for this virus. The potential vector/s for this virus has not been identified, but is likely to be mites or nematodes which are known to transmit other members of the genus. The identification of vectors will be investigated in future work. Infected *N. benthamiana* plants showed mild symptoms with a yellowing of infected leaves, and then recovered relatively quickly (10 days). When infected leaf tissue was examined for potential cytopathological effects, no morphological changes were observed in the nuclei of cells from infected plants. However, chloroplasts were observed to be mildly swollen and to contain more starch granules compared to those in non-inoculated leaves. Changes in chloroplast structure are typical of viral infections and depend on the severity of symptoms (Bhattacharyya & Chakraborty, 2018; Zhao et al., 2016), which explains why only small effects were observed in CuNVA here. In addition, specific circular membranous structures were observed in the cytoplasm which could correspond to viral factories or inclusion bodies, as has been described before for other nepoviruses (Roberts & Harrison, 1970). Nevertheless, the most characteristic effect of this virus was observed in the cytoplasm and plasmodesmata. Membranous structures containing rows of isometrical particles of around 25 nm (possibly viral particles) were observed in the cytoplasm close to the cellular membrane. These structures appeared to be produced in the cytoplasm and then potentially use plasmodesmata to move to neighbouring cells as shown previously for other nepoviruses such as strawberry latent ringspot virus and grapevine fanleaf virus (Ritzenthaler, 1995; Roberts & Harrison, 1970). Therefore, CuNVA appears to have all the basic features of a typical nepovirus though further studies are necessary to understand the mode of transmission, the epidemiology as well as the host range of this virus.

Cucumbers are an economically important crop cultivated in numerous countries around the world (Paris et al., 2012; Sebastian et al., 2010). Using a HTS approach we have identified several viruses previously identified from cucumbers in Greece (including Crete), present in samples with mixed virus infections. The results highlight the prevalence of mixed virus infections which can induce a range of symptoms in host plants. HTS can rapidly allow shifts in the major viruses impacting production areas to be identified and enable the implementation of additional diagnostic screening in commercial production areas. The HTS data revealed near-complete genomes of several species, with ZYFV selected for complete characterisation based on published sequence data at the time of the study. In addition to detecting known viruses, we have sequenced the complete genome of a novel nepovirus, named CuNVA. This highlights the additional power of using HTS, with novel viruses detected in addition to previously characterised species.

ACKNOWLEDGEMENTS

The authors thank the local social cooperative enterprise ‘Melitakes’ (https://melitakes.gr) located in Pyrgos, Heraklion, Greece and especially Stella Hatzigeorgiou for sample K96i, as well as Messaras Agricultural School/Maria Halkiadaki for samples GS1 and GS2. We would also like to thank Sevasti Papadogiorgaki for technical assistance with TEM, Mary Providaki and Anastasia Nikoloudi for technical support, and Chrysoula Orphanidou and Varvara Maliogka for kindly sharing with us primers p25_CYSDV_F/p25_CYSDV_R. Samples for this project were collected through the General Secretariat of Research and Technology Project 'Emblematic Action for Research in the Cretan Agrofood Sector: Four Institutions, Four References' (Agro4Crete – 2018SE01300000). This work was funded by the European Union- Next Generation EU, Greece 2.0 National Recovery and Resilience plan, National Flagship Initiative "Innovations in Plant Protection for sustainable and environmentally friendly pest control" InnoPP – TAEDR-0535675.

CONFLICT OF INTEREST STATEMENT

The authors declare no competing interests.

DATA AVAILABILITY STATEMENT

Data from this work have been uploaded in SRA (NCBI) under the following ID: PRJNA1076685.

ORCID

Anthony James https://orcid.org/0000-0003-4573-932X

Konstantina Katsarou https://orcid.org/0000-0003-2728-443X

REFERENCES

Adams, M. J., Antoniw, J. F., & Beaudoin, F. (2005). Overview and analysis of the polyprotein cleavage sites in the family Potyviridae. *Molecular Plant Pathology*, *6*, 471–487.

Andrews, S. (2010). FastQC: A quality control tool for high throughput sequence data. http://www.bioinformatics.babraham.ac.uk/projects/fastqc

Antignus, Y., Levy, D., & Cohen, S. (1995). Characterisation of a variant of zucchini yellow fleck virus (ZYFV), a potyvirus causing a wilt disease of melons in Israel. *Annals of Applied Biology*, *126*, 111–120.

Avgelis, A. D. (1983). Occurrence of Watermelon mosaic virus 1 and 2 in cucurbits in Crete (Greece)/Presenza dei virus 1 e 2 del mosaico dell'Anguria su cucurbitacee a Creta (Grecia). *Phytopathologia Mediterranea*, *22*, 219–221.

Avgelis, A. D. (1985). Epidemiological studies of zucchini yellow fleck virus in Crete. *Phytopathologia Mediterranea*, *24*, 208–210.

Avgelis, A. D., & Vovlas, C. (1986). Occurrence of cucumber green mottle mosaic virus in the Island of Crete (Greece)/Il virus della maculatura verde del Cetriolo a Creta (Grecia). *Phytopathologia Mediterranea*, *25*, 166–168.

Avgelis, A. D., & Vovlas, C. (1989). Artichoke yellow ringspot nepovirus naturally infecting cucumber in Crete. *Netherlands Journal of Plant Pathology*, *95*, 177–184.

Bananej, K., & Vahdat, A. (2008). Identification, distribution and incidence of viruses in field-grown cucurbit crops of Iran. *Phytopathologia Mediterranea*, *47*, 247–257.

Bhattacharyya, D., & Chakraborty, S. (2018). Chloroplast: The Trojan horse in plant–virus interaction. *Molecular Plant Pathology*, *19*, 504–518.

Boubourakas, I. N., Avgelis, A. D., Kyriakopoulou, P. E., & Katis, N. I. (2006). Occurrence of yellowing viruses (*Beet pseudo-yellows virus*, *Cucurbit yellow stunting disorder virus* and *Curcubit aphid-borne yelows virus*) affecting curcubits in Greece. *Plant Pathology*, *55*, 276–283.

Bushnell, B. (n.d.). BBmap. https://sourceforge.net/projects/bbmap/, https://sourceforge.net/projects/bbmap/

Camacho, C., Coulouris, G., Avagyan, V., Ma, N., Papadopoulos, J., Bealer, K., & Madden, T. L. (2009). BLAST+: Architecture and applications. *BMC Bioinformatics*, *10*, 1–9.

Chen, S., Zhou, Y., Chen, Y., & Gu, J. (2018). Fastp: An ultra-fast all-in-one FASTQ preprocessor. *Bioinformatics*, *34*, i884–i890.

Chu, P. W. G., Francki, R. I. B., & Hatta, T. (1983). Some properties of tomato ringspot virus isolated from *Pentas lanceolata* in South Australia. *Plant pathology*, *32*, 353–356.

Chung, B. Y.-W., Miller, W. A., Atkins, J. F., & Firth, A. E. (2008). An overlapping essential gene in the Potyviridae. *Proceedings of the National Academy of Sciences of the United States of America*, *105*, 5897–5902.

Desbiez, C. (2020). The never-ending story of cucurbits and viruses. *Acta Horticulturae*, *1294*, 173–192.

Desbiez, C., Justafre, I., & Lecoq, H. (2007). Molecular evidence that zucchini yellow fleck virus is a distinct and variable potyvirus related to papaya ringspot virus and Moroccan watermelon mosaic virus. *Archives of Virology*, *152*, 449–455.

Felsenstein, J. (1985). Confidence limits on phylogenies: An approach using the bootstrap. *Evolution*, *39*, 783–791.

Fuchs, M., Schmitt-Keichinger, C., & Sanfaçon, H. (2017). A renaissance in Nepovirus research provides new insights into their molecular Interface with hosts and vectors. *Advances in Virus Research*, *97*, 61–105.

Gan, GQ., Chang-fa, C., Yingchao, W., Ying, J., Xing-hai, W., & Xiuling, S. (2013). Detection and identification of tomato black ring Nepovirus from imported cucumber seeds. *Food Research and Development*, *34*, 88–90.

Gilbert-Albertini, F., & Lecoq, H. (1994). The characterization of a strain of zucchini yellow fleck virus found in southeastern France. *Journal of Phytopathology*, *140*, 375–384.

Goh, C. J., & Hahn, Y. (2021). Analysis of proteolytic processing sites in potyvirus polyproteins revealed differential amino acid preferences of NIa-pro protease in each of seven cleavage sites. *PLoS One*, *16*, e0245853.

Goodacre, N., Aljanahi, A., Nandakumar, S., Mikailov, M., & Khan, A. S. (2018). A reference viral database (RVDB) to enhance bioinformatics analysis of high-throughput sequencing for novel virus detection. *mSphere*, *3*, e00069–e00118.

Hall, B. G. (2013). Building phylogenetic trees from molecular data with MEGA. *Molecular Biology and Evolution*, *30*, 1229–1235.

Harrison, B. D., Finch, J. T., Gibbs, A. J., Hollings, M., Shepherd, R. J., Valenta, V., & Wetter, C. (1971). Sixteen groups of plant viruses. *Virology*, *45*, 356–363.

Hily, J. M., Poulicard, N., Kubina, J., Reynard, J. S., Spilmont, A. S., Fuchs, M., Lemaire, O., & Vigne, E. (2021). Metagenomic analysis of nepoviruses: Diversity, evolution and identification of a genome region in members of subgroup a that appears to be important for host range. *Archives of Virology*, *166*, 2789–2801.

Katsarou, K., Mitta, E., Bardani, E., Oulas, A., Dadami, E., & Kalantidis, K. (2018). DCL-suppressed *Nicotiana benthamiana* plants : Valuable tools in research and biotechnology. *Molecular Plant Pathology*, *20*, 432–446.

Katul, L., & Makkouk, K. (1987). Occurence and serological relatedness of five cucurbit potyviruses in Lebanon and Syria. *Phytopathologia Mediterranea*, *26*, 36–42.

Kumar, S., Stecher, G., Li, M., Knyaz, C., & Tamura, K. (2018). MEGA X: Molecular evolutionary genetics analysis across computing platforms. *Molecular Biology and Evolution*, *35*, 1547–1549. https://doi.org/10.1093/molbev/msy096

Lu, S., Wang, J., Chitsaz, F., Derbyshire, M. K., Geer, R. C., Gonzales, N. R., Gwadz, M., Hurwitz, D. I., Marchler, G. H., Song, J. S., Thanki, N., Yamashita, R. A., Yang, M., Zhang, D., Zheng, C., Lanczycki, C. J., & Marchler-Bauer, A. (2020). CDD/SPARCLE: The conserved domain database in 2020. *Nucleic Acids Research*, *48*, D265–D268.

Martin, D. P., Murrell, B., Golden, M., Khoosal, A., & Muhire, B. (2015). RDP4: Detection and analysis of recombination patterns in virus genomes. *Virus Evolution*, *1*, vev003.

Moore, B. J., & McGuire, J. M. (1968). Translocation of tobacco ringspot virus in cucumber and Zinnia. *Arkansas Academy of Science Proceedings*, *22*, 67–71. https://scholarworks.uark.edu/jaas/vol22/iss1/14

Muhire, B. M., Varsani, A., & Martin, D. P. (2014). SDT: A virus classification tool based on pairwise sequence alignment and identity calculation. *PLoS One*, *9*, e108277.

Orfanidou, C., Maliogka, V. I., & Katis, N. I. (2014). First report of cucurbit chlorotic yellows virus in cucumber, melon, and watermelon in Greece. *Plant Disease*, *98*, 1446.

Orfanidou, C. G., Beta, C., Reynard, J. S., Tsiolakis, G., Katis, N. I., & Maliogka, V. I. (2020). Identification, molecular characterization and prevalence of a novel cytorhabdovirus infecting zucchini crops in Greece. *Virus Research*, *287*, 198095.

Orfanidou, C. G., Papayiannis, L. C., Pappi, P. G., Katis, N. I., & Maliogka, V. I. (2019). Criniviruses associated with cucurbit yellows disease in Greece and Cyprus: An ever-changing scene. *Plant Pathology*, *68*, 764–774.

Palukaitis, P., Roossinck, M. J., Dietzgen, R. G., & Francki, R. I. B. (1992). Cucumber mosaic virus. *Advances in Virus Research*, *41*, 281–348.

Paris, H. S., Daunay, M. C., & Janick, J. (2012). Occidental diffusion of cucumber (*Cucumis sativus*) 500–1300 CE: Two routes to Europe. *Annals of Botany*, *109*, 117–126.

Prjibelski, A., Antipov, D., Meleshko, D., Lapidus, A., & Korobeynikov, A. (2020). Using SPAdes De Novo Assembler. *Current Protocols in Bioinformatics*, *70*, e102.

Ritzenthaler, C. (1995). Grapevine Fanleaf Nepovirus P38 putative movement protein is located on tubules *in vivo*. *Molecular Plant-Microbe Interactions*, *8*, 379.

Roberts, I. M., & Harrison, B. D. (1970). Inclusion bodies and tubular structures in *Chenopodium amaranticolor* plants infected with strawberry latent ringspot virus. *Journal of General Virology*, *7*, 47–54.

Saitou, N., & Nei, M. (1987). The neighbor-joining method: A new method for reconstructing phylogenetic trees. *Molecular Biology and Evolution*, 4(4), 406–425. https://doi.org/10.1093/oxfordjournals.molbev.a040454

Sanfaçon, H. (2008). Nepovirus. In *Encyclopedia of virology* (3rd ed., pp. 405–413). Academic Press.

Sanfaçon, H. (2022). Re-examination of nepovirus polyprotein cleavage sites highlights the diverse specificities and evolutionary relationships of nepovirus 3C-like proteases. *Archives of Virology*, *167*, 2529–2543.

Sareli, K., Winter, S., Chatzivassiliou, E., Knierim, D., & Margaria, P. (2022). High molecular diversity of full-length genome sequences of zucchini yellow fleck virus from Europe. *Archives of Virology*, *167*, 2305–2310.

Scotto–Lavino, E., Du, G., & Frohman, M. A. (2006a). 3′ end cDNA amplification using classic RACE. *Nature Protocols*, *1*, 2742–2745.

Scotto–Lavino, E., Du, G., & Frohman, M. A. (2006b). 5′ end cDNA amplification using classic RACE. *Nature Protocols*, *1*, 2555–2562.

Sebastian, P., Schaefer, H., Telford, I. R. H., & Renner, S. S. (2010). Cucumber (*Cucumis sativus*) and melon (*C. Melo*) have numerous wild relatives in Asia and Australia, and the sister species of melon is from Australia. *Proceedings of the National Academy of Sciences of the United States of America*, *107*, 14269–14273.

Tomassoli, L., Tiberini, A., & Meneghini, M. (2010). *Zucchini yellow fleck virus* is an emergent virus on melon in Sicily (Italy). *Journal of Phytopathology*, *158*, 314–316.

Tomitaka, Y., Usugi, T., Yasuda, F., Okayama, H., & Tsuda, S. (2011). A novel member of the genus *Nepovirus* isolated from *Cucumis melo* in Japan. *Phytopathology*, *101*, 316–322.

Vovlas, C., Hiebert, E., & Russo, M. (1981). Zucchini yellow fleck virus, a new potyvirus of zucchini squash. *Phytopathologia Mediterranea*, *20*, 123–128.

Yang, X., Li, Y., & Wang, A. (2021). Research advances in Potyviruses: From the laboratory bench to the field. *Annual Review of Phytopathology*, *59*, 1–29.

Zhao, J., Zhang, X., Hong, Y., & Liu, Y. (2016). Chloroplast in plant-virus interaction. *Frontiers in Microbiology*, *7*, 1565. doi:10.3389/fmicb.2016.01565. http://journal.frontiersin.org/article

SUPPORTING INFORMATION

Additional supporting information can be found online in the Supporting Information section at the end of this article.

How to cite this article: James, A., Kryovrysanaki, N., Andronis, C., Pappi, P. G., Kalantidis, K., & Katsarou, K. (2025). Identification and characterisation of *Zucchini yellow fleck virus* and a novel *Nepovirus* from next-generation sequencing of mixed virus infections in cucumbers (*Cucumis sativus*) from Crete. *Annals of Applied Biology*, *186*(3), 248–261. https://doi.org/10.1111/aab.12962